



Syntheses and characterization of several nickel bis(dithiolene) complexes with strong and broad Near-IR absorption

Qingqing Miao, Junxiong Gao, Zeqing Wang, Hang Yu, Yi Luo, Tingli Ma^{*}

State Key Laboratory of Fine Chemicals, School of Chemical Engineering, Dalian University of Technology, Dalian 116024, China

ARTICLE INFO

Article history:

Received 11 May 2011

Received in revised form 22 July 2011

Accepted 27 July 2011

Available online 2 August 2011

Keywords:

NIR dye

Nickel bis(dithiolene) complex

Crystal stacking

Optical spectroscopy

Photoelectrochemistry

ABSTRACT

Several nickel bis(dithiolene) complexes with strong and broad absorptions in the Near-IR (NIR) region (700–1100 nm) were synthesized by using green and simple synthetic routes. The physical and chemical properties of these dyes were systematically studied, including structure, optical spectroscopy and electrochemical behavior, etc. These NIR dyes were first applied to dye-sensitized solar cells (DSCs) and the photoelectrochemical performances were also investigated. The effects of different substituent groups on the properties of the dyes and photovoltaic performances of DSCs were discussed. Furthermore, we also applied the synthesized NIR dyes for constructing NIR absorbing filter. With their particular photoelectrochemical properties, the nickel bis(dithiolene) complexes exhibit promising prospects for future application.

© 2011 Elsevier B.V. All rights reserved.

1. Introduction

Nickel bis(dithiolene) complexes are important Near-IR (NIR) dyes [1]. They have attracted much attention due to their unique optical, electronic, magnetic, and electrochemical properties [2–4]. With these particular properties, such as superior photostability, air-stability, thermal stability, tense and broad absorption in the NIR region, easy adjustment of the absorption range, high molecular absorption coefficient [5] and high electron mobility [6], many applications have been developed. They have been used as NIR photodetectors, Q-switch dye lasers, antioxidants for polymers, light stabilizers, laser diodes for optical switching devices [5,7–18]. However, there is little systematic research on the synthesis and characterizations of the nickel bis(dithiolene) complexes. In addition, as we know, there is no report on the application in the field of dye-sensitized solar cell (DSC).

DSC is a new type of photovoltaic cell [19]. It has attracted considerable interest due to its unique advantages, such as high efficiency, low cost and the simple fabrication process. For successful commercialization, it is necessary to further improve the energy conversion efficiency of DSC. Many attempts have been carried out, however, the results are not satisfying. One of the most effective methods for further improving the efficiency is broadening the absorption spectra of the cells and utilizing the NIR light, which is 45% of the

total solar energy. The theoretical calculation has proved that the efficiency of DSCs will be greatly improved with the broadened absorption spectrum [20]. Kuster et al. reported the squaraine NIR dye for DSC [21]. Mori et al. also reported the DSC based on zinc phthalocyanine, with the efficiency of 4.6% [22]. The above results exhibit the promising prospects of NIR dyes for DSC. Furthermore, the NIR dyes can be used in tandem DSCs, hybrid DSCs and co-sensitized DSCs [23–25]. Our group has successfully developed a new type of hybrid DSC by using a NIR dye (zinc phthalocyanine) and a visible dye (pyrazine-dicarboxylic acid) [26]. However, the problems of the NIR dyes currently used for DSCs are the narrow absorption bands (the end of the absorption band is usually below 800 nm) and the low efficiencies. Therefore, it is necessary to develop NIR dyes with strong and broad absorptions between 800 and 1200 nm for DSCs.

In this work, several nickel bis(dithiolene) complexes with strong and broad absorptions were synthesized and the structures were shown in Fig. 1(A–D). The synthesis of A and B were performed using the modified green synthetic routes. C and D were synthesized by another simple method, especially the synthetic route of C and D is first reported. We also systematically studied the properties of optical spectroscopy and electrochemistry of these complexes. These synthesized nickel bis(dithiolene) complexes were first applied to DSCs. The effects of the different substituent groups on the photovoltaic performances of DSCs and the energy level matching were investigated. Furthermore, the application of the complex for NIR absorbing filter was also conducted.

^{*} Corresponding author. Tel.: +86 411 84986237; fax: +86 411 84986230.
E-mail address: tinglima@dlut.edu.cn (T. Ma).

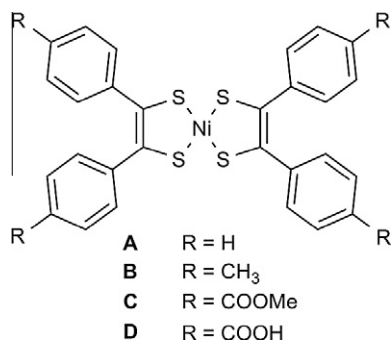


Fig. 1. Structures of the nickel bis(dithiolene) complexes.

2. Experimental

2.1. General analytical measurements

¹H NMR spectra were taken with a Bruker Avance|–400 NMR spectrometer (Switzerland). Chemical shifts were referenced to TMS(Me₄Si) and expressed as δ (ppm) values. IR spectra were measured in KBr pellets with a Nicolet Nexus (USA) FT-IR instrument in the range of 4000–400 cm⁻¹. Element analysis was recorded with a vario EL III analyzer. All chemicals were commercially available and were used without further purification.

2.2. Synthesis and characterization

2.2.1. Synthesis of bis(1,2-diphenylethylene-1,2-dithiolate) nickel complex (A)

2.2.1.1. Preparation of benzoin (2) [27]. A mixture of thiamine (VB₁, 3.31 g, 11 mmol), distilled water (7 ml) and 95% ethanol (30 ml) was stirred and cooled in the ice-water bath. The precooled 10% NaOH solution (10 ml) and fresh benzaldehyde (compound **1**, 21.22 g, 200 mmol) were slowly added to the mixture in turn. After stirring, the obtained mixture was refluxed at 70 °C for 1.5 h in the pH of 9–10. The hot reaction mixture was allowed to cool down to room temperature and then immersed in an ice-water bath overnight. The yellowish powder was collected by filtration and the crude product was washed with water several times. Purification was performed by recrystallization from 95% ethanol to give 12.69 g of white crystals (compound **2**), yield 59.8%; ¹H NMR (400 MHz, CDCl₃/TMS, δ /ppm, J/Hz) δ : 4.54 (s, 1H), 5.95 (s, 1H), 7.27–7.42 (m, 7H), 7.50–7.54 (m, 1H), 7.91 (d, J = 8.54 Hz, 2H). FT-IR (KBr, cm⁻¹) ν : 3414, 3378, 3083, 3059, 3028, 2932, 1679, 1595, 1578, 1490, 1449, 1262, 1207, 1068, 755, 704.

2.2.1.2. Preparation of complex A [28]. Benzoin (2.12 g, 10 mmol) was refluxed with P₂S₅ (3.33 g, 15 mmol) in 30 ml of dioxane for 10 h. During this period, the thiophosphoric ester of dithiobenzoin was formed. The hot reaction mixture was filtered to remove the excess P₂S₅ and a solution of NiCl₂·6H₂O (1.16 g, 4.9 mmol) in 8 ml distilled water was added to the filtrate. The reaction mixture was refluxed for 2–4 h and cooled by an ice-water bath. Green-black crystal of the complex was formed and collected by filtration, washed with a minimal amount of dioxane, water, ethanol, and ether. It was then dried to give a crude complex A. Purification was conducted by recrystallization from dichloromethane to afford 1.63 g of green-black rod-like crystals (complex A), yield 60.0%; ¹H NMR (400 MHz, CDCl₃/TMS, δ /ppm, J/Hz) δ : 7.29 (d, J = 7.47 Hz, 4H), 7.31 (d, J = 7.47 Hz, 4H), 7.37–7.38 (m, 8H), 7.39–7.40 (m, 4H). ¹³C NMR (100 MHz, CDCl₃, δ /ppm) δ : 128.40 (aryl carbon), 128.93 (aryl carbon), 128.96 (aryl carbon), 141.21 (aryl carbon), 181.64 (vinyl carbon). FT-IR (KBr, cm⁻¹) ν : 1571, 1493, 1442,

1361, 1138, 882, 749, 696, 407. Anal. Calc. for C₂₈H₂₀NiS₄: C, 61.89; H, 3.71; S, 23.60. Found: C, 61.55; H, 3.55; S, 23.20%. UV-Vis (CH₂Cl₂, nm) λ_{\max} (ϵ): 270 (38 306), 317 (53 182), 598 (2 219), 857 (33 885).

2.2.2. Synthesis of bis [1,2-di(4-methylphenyl)ethylene-1,2-dithiolate] nickel complex (B)

2.2.2.1. Preparation of 4,4'-dimethylbenzil (5). Compound **5** was prepared by an improved procedure analogous to that for 4,4'-disubstituted benzil [29]. In a mechanically stirred and CaCl₂ drying tube dried suspension of anhydrous aluminum chloride (3.33 g, 25 mmol) and toluene (10.6 ml, 100 mmol, as the reactant and solvent) at 0–5 °C was slowly added to oxalyl chloride (1.27 g, 10 mmol) in 5 ml toluene. The rufous reaction mixture was stirred for 2 h and continued for another 10 h at room temperature. The resulting mixture was quenched with crushed ice (20 g) mixed with concentrated hydrochloric acid (2 ml). The organic phase was separated and the aqueous phase was extracted with petroleum ether. The combined organic phases were washed with water, saturated NaHCO₃, water again and then dried over anhydrous Na₂SO₄. The solvent was removed in vacuum and the residue was purified by recrystallization from 95% ethanol to give 1.67 g of faint red sheet crystals (compound **5**), yield 70.2%; ¹H NMR (400 MHz, d₆-DMSO, δ /ppm, J/Hz) δ : 3.33 (s, 6H), 7.43 (d, J = 8.08 Hz, 4H), 7.80 (d, J = 8.08 Hz, 4H). FT-IR (KBr, cm⁻¹) ν : 2917, 1661, 1604, 1173, 830, 746.

2.2.2.2. Preparation of complex B [30]. Compound **5** (1.19 g, 5 mmol) was refluxed with P₂S₅ (1.67 g, 7.5 mmol) in 15 ml of dioxane for 6 h. During this period, the thiophosphoric ester was formed. The red brown reaction mixture was filtered to remove the excess P₂S₅ and a solution of NiCl₂·6H₂O (0.58 g, 2.5 mmol) in 2.3 ml distilled water was added to the filtrate. The reaction mixture was refluxed for 2–4 h and cooled by an ice-water bath. The dark green crystal of the complex was formed and collected by filtration, washed with a minimal amount of dioxane, water, ethanol, ether, and then dried to give the crude complex B. Purification is effected by recrystallization from dichloromethane to afford 0.93 g of dark green solid (complex B), yield 62.1%; ¹H NMR (400 MHz, CDCl₃/TMS, δ /ppm, J/Hz) δ : 2.33 (s, 12H), 7.09 (d, J = 8.10 Hz, 8H), 7.29 (d, J = 8.10 Hz, 8H). ¹³C NMR (100 MHz, CDCl₃, δ /ppm) δ : 21.46 (methyl carbon), 128.80 (aryl carbon), 129.12 (aryl carbon), 138.69 (aryl carbon), 139.04 (aryl carbon), 181.35 (vinyl carbon). FT-IR (KBr, cm⁻¹) ν : 2972, 2916, 1603, 1407, 1358, 1141, 887, 807, 408. Anal. Calc. for C₃₂H₂₈NiS₄: C, 64.11; H, 4.71; S, 21.39. Found: C, 63.72; H, 4.54; S, 21.29%. UV-Vis (CH₂Cl₂, nm) λ_{\max} (ϵ): 276 (32 279), 320 (36 866), 600 (1 704), 884 (27 655).

2.2.3. Synthesis of bis [1,2-di(4-methoxycarbonylphenyl)ethylene-1,2-dithiolate] nickel complex (C)

2.2.3.1. Preparation of 4,4'-bis(methyloxycarbonyl)benzoin (7). Compound **7** was synthesized by an improved scheme, combining the two methods in previous studies [31,32]. Potassium cyanide (0.98 g, 15 mmol) was added to the solution of methyl 4-formylbenzoate (**6**) (8.21 g, 50 mmol) stirred in 99% ethanol (35 ml) and water (9 ml). The reaction mixture was stirred at 30 °C for 15 min. The product was collected by filtration, washed with water, dried under reduced pressure, and recrystallized from ethanol to give 6.70 g of pale yellow needles, yield 81.6%; ¹H NMR (400 MHz, d₆-DMSO, δ /ppm, J/Hz) δ : 3.81 (s, 3H), 3.86 (s, 3H), 6.17 (s, 1H), 6.48 (s, 1H), 7.55 (d, J = 8.30 Hz, 2H), 7.90 (d, J = 8.30 Hz, 2H), 8.01 (d, J = 8.50 Hz, 2H), 8.10 (d, J = 8.50 Hz, 2H).

2.2.3.2. Preparation of complex C. Complex C was synthesized by our methods. Compound **7** (0.98 g, 3 mmol) was refluxed with P₂S₅ (0.10 g, 4.5 mmol) in 8 ml of dioxane for 8 h. During this period,

the thiophosphoric ester was formed. The red brown reaction mixture was filtered to remove the excess P_2S_5 and a solution of $NiCl_2 \cdot 6H_2O$ (0.36 g, 1.5 mmol) in 2 ml distilled water was added to the filtrate. The reaction mixture was refluxed for 2 h, cooled by an ice-water bath, and concentrated to remove the solvent. The residue was collected by filtration, washed with a minimal amount of dioxane, water, ethanol, ether, and dried to give the crude product. Purification was performed by column chromatography using silica gel and dichloromethane–petroleum ether mixture (1/1; v/v) as the eluent to give 0.23 g of bottle green solid (complex C), yield 19.8%; 1H NMR (400 MHz, $CDCl_3/TMS$, δ/ppm , J/Hz): 4.30 (s, 12H), 7.41 (d, $J = 8.26$ Hz, 8H), 8.12 (d, $J = 8.26$ Hz, 8H). FT-IR (KBr, cm^{-1}): 2924, 2853, 1717, 1637, 1596, 1464, 1404, 1363, 1355, 1273, 1230, 1142, 1113, 1064, 1014, 889, 805, 409. Anal. Calc. for $C_{36}H_{28}NiO_8S_4$: C, 55.75; H, 3.64; S, 16.54. Found: C, 55.70; H, 3.58; S, 16.42%. UV–Vis (CH_2Cl_2 , nm) λ_{max} (ϵ): 261 (19 284), 328 (40 909), 601 (1034), 868 (18 518).

2.2.4. Synthesis of bis [1,2-di(4-carboxylphenyl)ethylene-1,2-dithiolate] nickel complex (D)

2.2.4.1. Preparation of 4,4'-bis(methyloxycarbonyl)benzil (8) [31]. 4.7 ml 48% aqueous hydrobromic acid was added slowly to the solution of 7 (3.28 g, 10 mmol) in DMSO (23 ml) under stirring. The solution was heated to 55 °C for 24 h followed by adding 25 ml water. The product was filtered, washed with water and dried at 70 °C in vacuum. Yield: 3.23 g (99%), yellow solid. 1H NMR (400 MHz, $CDCl_3/TMS$, δ/ppm , J/Hz): 3.99 (s, 6H), 8.07 (d, $J = 8.15$ Hz, 4H), 8.20 (d, $J = 8.15$ Hz, 4H).

2.2.4.2. Preparation of 4,4'-bis(hydroxycarbonyl)benzil (9) [31]. The mixture of 8 (1.6 g, 4.9 mmol) in acetic acid (120 ml) and a 4:1 H_2SO_4/H_2O solution (55 ml) was refluxed and stirred for 10 h. Then 80 ml water was added and the mixture solution was cooled on ice. The filtration was performed. The product was washed with water, and dried at 70 °C in vacuum. Yield: 1.4 g (96%), pale yellow solid. 1H NMR (400 MHz, DMSO/TMS, δ/ppm , J/Hz): 8.08 (d, $J = 8.20$ Hz, 4H), 8.15 (d, $J = 8.20$ Hz, 4H), 13.38 (s, 2H).

2.2.4.3. Preparation of bis [1,2-di(4-carboxylphenyl)ethylene-1,2-dithiolate] nickel complex (D). Compound 9 (0.89 g, 3 mmol) was refluxed with P_2S_5 (0.10 g, 4.5 mmol) in 8 ml of dioxane for 8 h. During this period, the thiophosphoric ester was formed. The red brown reaction mixture was filtered to remove the excess P_2S_5 and a solution of $NiCl_2 \cdot 6H_2O$ (0.36 g, 1.5 mmol) in 2 ml distilled water was added to the filtrate. The reaction mixture was refluxed for 2 h, cooled by an ice-water bath, and concentrated to remove the solvent. The residue was collected by filtration, washed with a minimal amount of dioxane, water, ethanol, ether, and dried to give the green product. 1H NMR (400 MHz, DMSO/TMS, δ/ppm , J/Hz): 8.07 (d, $J = 8.37$ Hz, 8H), 8.14 (d, $J = 8.37$ Hz, 8H), 13.54 (s, 4H). FT-IR (KBr, cm^{-1}): 3429, 1670, 1596, 1404, 1268, 1204, 1174, 1047, 881, 840, 730, 696, 405. UV–Vis (CH_2Cl_2 , nm) λ_{max} : 315, 595, 890.

2.3. X-ray crystal structure determination

X-ray crystal structures were characterized by Bruker Smart APEXII (Germany) CCD X-ray single crystal diffractometer. The structures were solved by the SHELXL software. Detailed crystal data and experimental parameters of complex B are given in Tables S1–S3 (Supplementary material).

2.4. Physical measurements

The UV–Vis–NIR absorption spectra were recorded using a HP8453 (USA) UV–Vis spectrophotometer in a 1×1 cm quartz absorption cell. The spectroelectrochemical measurements were

performed at room temperature using an OTTLE cell with a Ag reference, a Pt counter and a Pt working electrode on a HP8453 (USA) UV–Vis spectrophotometer. The CH_2Cl_2 solution was degassed by bubbling argon through the cell for 10 min and tetrabutylammonium hexafluorophosphate ($[^nBu_4N][PF_6]$, TBAHFP, Fluka, puriss electrochemical grade, $\geq 99.0\%$) was used as supporting electrolyte in a small ArCN solution. The bias was performed by a computer controlled potentiostat (Zenium, Zahner, Germany). Electrochemical measurements were carried out on a BAS100W (USA) electrochemistry workstation at room temperature under argon, using 1 mM analyte in dry, deoxygenated dichloromethane (distilled from CaH_2) solution, supporting electrolyte (0.1 M $[^nBu_4N][PF_6]$), a glassy carbon working electrode, a Pt auxiliary electrode, an Ag/AgCl reference electrode. The scan rate was 100 mV/s. Ferrocene was added and the ferrocenium/ferrocene (Fc^+/Fc) redox couple was used as the internal reference for calibration. The geometrical and electronic properties of the dyes were performed with DFT calculations using the GAUSSIAN 03 software by B3LYP and 6-31G (d). Current–voltage (I – V) curves of DSCs were conducted by a Keithley digital source meter (Keithley 2601, USA) under a 300 W solar simulator simulating the AM 1.5 spectrum (100 mW/cm², Solar Light Co., Inc., USA). The incident light intensity was calibrated with a solar power meter (TES-1333R, Taiwan) and a standard amorphous silicon solar cell (BS-520, Bunkoh-Keiki Co., Ltd., Japan).

2.5. Fabrication of DSCs

The TiO_2 paste of commercial P25 powder (Degussa) using polyethylene glycol 600 (PEG 600) as a dispersant was prepared, according to the procedure developed by our group [33]. A screen-printing method was used to fabricate TiO_2 films on the cleaned fluorine-doped tin oxide conducting glass (FTO glass, Asahi Glass Co. Ltd.; sheet resistance: 10 ohm/square). The obtained electrodes coated with the TiO_2 paste were sintered at 500 °C for 30 min. While cooling to 40 °C, they were immersed into the dye solutions and kept at room temperature for 20 h. The dye solutions of the three nickel bis(dithiolene) complexes were saturated solutions dissolved in dichloromethane. A sandwich cell was prepared using the dye sensitized TiO_2 film (15 μ m, 0.2 cm²), a Pt-sputtered FTO counter electrode and the electrolyte containing 0.03 M I_2 , 0.06 M LiI, 0.6 M 1,2-dimethyl-3-propylimidazolium iodine (BMII), 0.1 M guanidinium thiocyanate and 0.5 M 4-*tert*-butylpyridine (4-TBP) in acetonitrile.

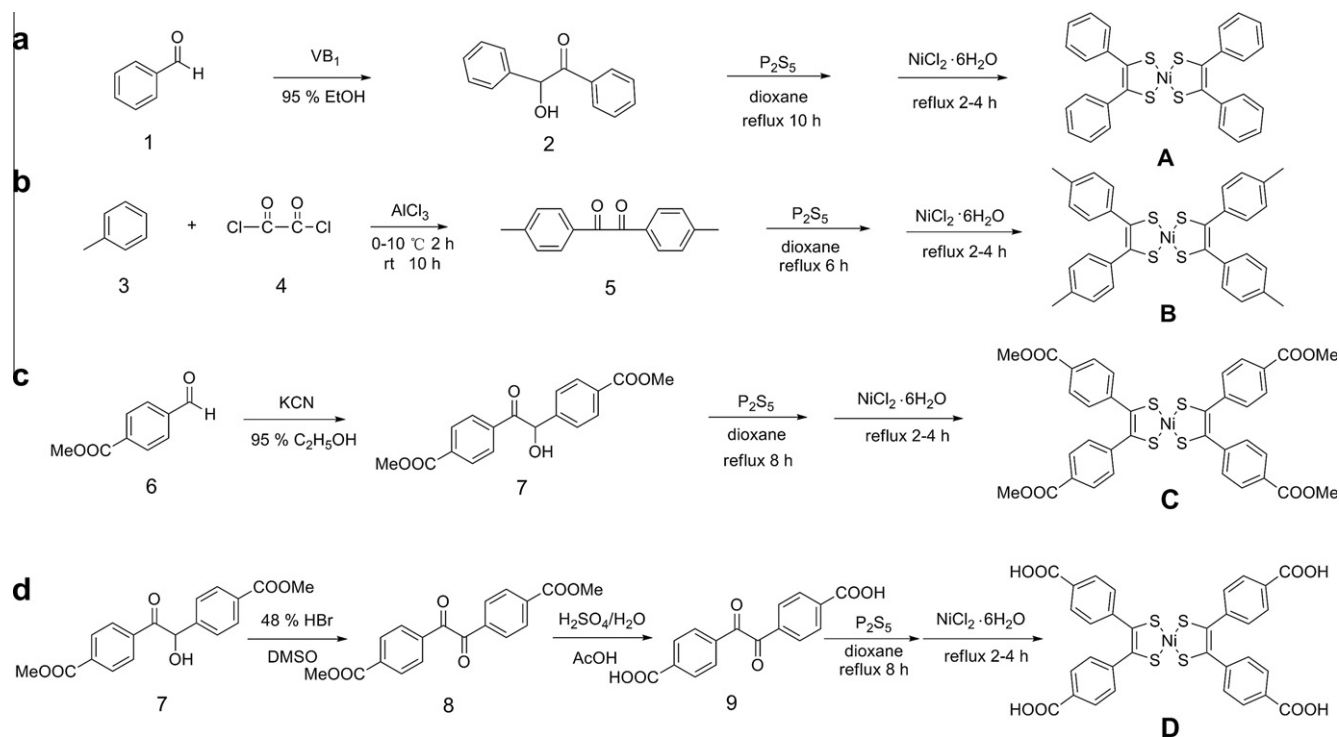
2.6. Fabrication of NIR absorbing filter

Polymethylmethacrylate (PMMA) was solved in CH_2Cl_2 to form a transparent and viscous solution, followed by adding the nickel bis(dithiolene) complex. After stirring, the solution was kept in vacuum and injected into the mold. The solvent was removed in the oven to afford the green NIR absorbing filter. For contrast, PMMA was fabricated in the same procedure without adding the nickel bis(dithiolene) complex.

3. Results and discussion

3.1. Synthesis

The nickel bis(dithiolene) complexes were synthesized by benzoin and benzil methods. A and C were obtained by benzoin methods, whereas B and D were afforded from benzil methods (Scheme 1). The synthesis of A and B were performed with corresponding benzoin or benzyl, which followed the modified green synthetic routes. When increasing the reflux time of the benzoin or benzyl



Scheme 1. The synthetic routes of (a) A, (b) B, (c) C, and (d) D.

with P_2S_5 , yields of the product were improved. There was no report on the syntheses of C and D. We found that it was difficult to obtain the corresponding complexes by the green synthetic routes. Finally, C and D were successfully obtained by a simple method as described in Scheme 1.

3.2. Structural properties

There are 10 π electrons for the nine atoms in the two five-membered rings of the molecule. The metal center provides the unoccupied orbital for the π -electron delocalization, which belongs to the Hückel ($4n + 2$) system.

The dark green rod-like single crystals of A, B, and C were obtained from the dichloromethane–hexane mixture. The crystal structures of A and B were determined. With the small needles, it was difficult to detect the X-ray crystal structure of C. The X-ray crystal structure of B is shown in Fig. 2. The crystal system is triclinic with the space group of $P\bar{1}$. A square-planar configuration

with a very limited tetrahedral distortion of B was found and all the distances of the four Ni–S bonds are equal within experimental error, which is consistent with the literature on the subject [34]. This means that the Ni center, four S atoms and two C=C are in a square-planar environment (plane Ni), which results in the π -conjugated delocalization of the nine atoms. The four Ni–S bonds are approximately equal (2.103(3)–2.108(3) Å) with the angles of nearly 90° for S–Ni–S. The average bond lengths for S–C and C=C are 1.692(5) and 1.390(6) Å, respectively. The benzyl groups are not in the same plane with the square-planar Ni–S–C ring, rather, they make torsion angles. The angles between the phenyl rings and the metallacycle are not identical, ranging from 36 – 44° (35.7° , 38.6° , 43.5° , 44.0°).

Fig. 3 shows the crystal stacking of A and B. Viewing along the a , b and c -axis, the varying but orderly projection views can be obtained for both A and B. The view of the unit cell of A shows that the plane Ni stack in order along the a -axis, in which the shortest intermolecular Ni...Ni distance is 5.955 Å. When it stacks along the b -axis and c -axis, the shortest distances change to 11.096 and 18.640 Å, corresponding to the cell parameters. The same conclusions can be made for the S...S and C...C in the plane. This further confirms the fact that all the nine atoms containing the Ni center, the four S atoms and the four C atoms are in the same plane. The shortest intra-stack Ni...Ni distance of 4.888 Å for B is obtained when it is stacked along the a -axis. However, the values are 11.395 and 15.220 Å while viewing along the b and c -axis, respectively.

3.3. IR spectra

The characteristic absorption peaks in the IR spectra of the complexes are similar. The peaks at ca. 1358 cm^{-1} can be assigned to the stretching vibration of C=C bonds (1361 cm^{-1} for A, 1358 cm^{-1} for B, 1355 cm^{-1} for C), whereas C=S bonds for A, B, and C were recorded at 1138 , 1141 and 1142 cm^{-1} , respectively. The peaks near 885 cm^{-1} originate from the stretching vibration

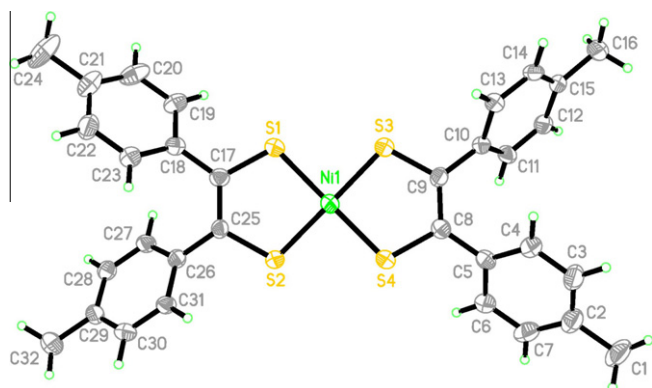


Fig. 2. The X-ray crystal structure of B.

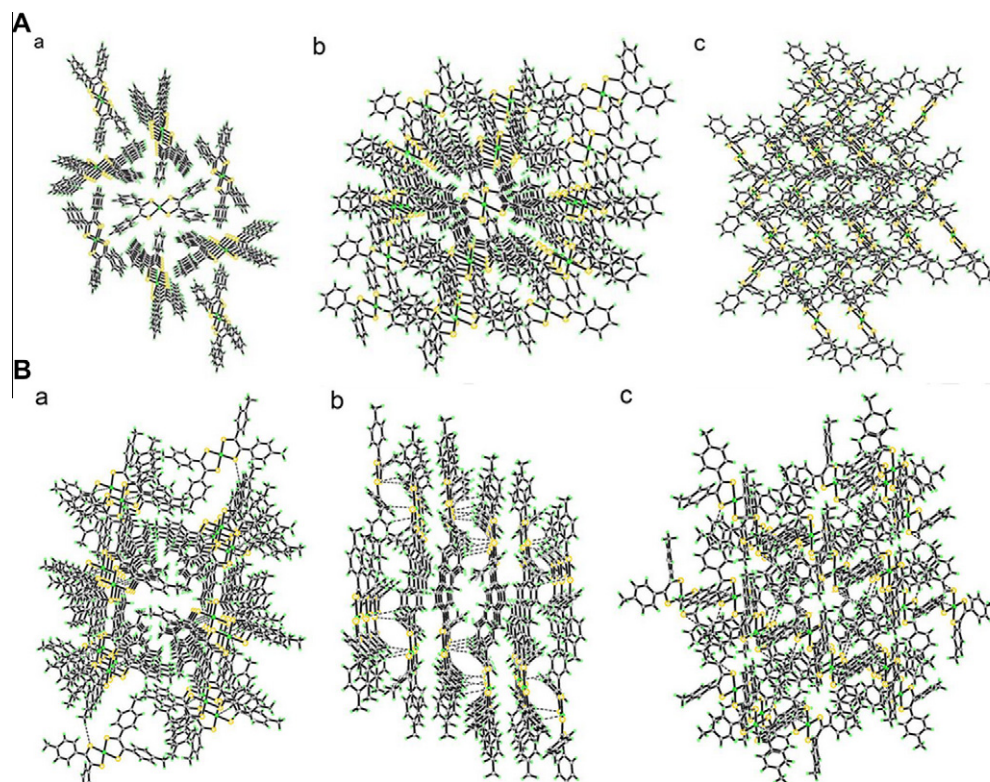


Fig. 3. Projection views of the unit cells of A (top) and B (bottom) along the *a*, *b* and *c*-axis. The distances between the atoms are calculated by the diamond software.

of the couple mode C=S and C–Ph. The Ni–S stretching bonds of A, B, and C appear at 407, 408 and 409 cm^{-1} , respectively. For complex A, the mono-substituted benzene peak appears at 749 and 696 cm^{-1} . The symbolized peaks for para-substituted benzene in B and C are 807 and 805 cm^{-1} , respectively. In addition, the peaks below 3000 cm^{-1} originate from the stretching vibrations of C–H of the methyl group. As for C, the peaks at 1457, 1363, 1273, and 1065 cm^{-1} are assigned to the bending vibration of C–H and stretching vibration of C–O in COOCH_3 [28].

3.4. UV–Vis–NIR spectra

3.4.1. The solvent effect

A, B, and C exhibit intense absorption bands below 400 nm and broad absorption bands with high molar extinction coefficients in the NIR region (700–1100 nm) (Fig. 4a). The bands below 400 nm originate from the ligand-to-metal charge-transfer (LMCT) bands and intraligand transitions [35]. The intense feature absorption bands in the NIR region are generally assigned to the $\pi \rightarrow \pi^*$ transition between HOMO and LUMO [36]. The λ_{max} values of A, B and C are 857, 884 and 868 nm, respectively. The high molar extinction coefficients are 33 885, 27 655, and 18 518 $\text{L mol}^{-1} \text{cm}^{-1}$, respectively.

The maximum absorption data of A, B, and C in different solvents are shown in Table 1. The positive solvatochromism is confirmed as increasing the polarity of the solvent. From this, one can interpret that the polar excited molecules of the complex are more susceptible to the solvation effect than ground state molecules when combined with the polar solvent, resulting in the lower energy of the excited molecules. Correspondingly, the decreased energy difference is achieved and the red-shifted λ_{max} can be observed. Furthermore, C suffers a larger effect when DMF and DMSO were used, causing the peak to fall to 944 nm in DMF and 957 nm in DMSO.

3.4.2. The substituent effect

Fig. 4a shows the effect of the functional group attached to benzene ring on the absorption maximum. It can be observed that the methyl-substituted phenyl derivative B exhibits the maximum absorption band at 884 nm in CH_2Cl_2 . It is red-shifted by 27 and 16 nm compared with H-substituted complex A and methoxycarbonyl-substituted phenyl derivative C, respectively. This can be explained by the fact that the methyl group, being the electron donating substituent, increases the electron density of the dithiolene moiety and decreases the gap of HOMO and LUMO, which then results in the red-shift of the NIR absorption maximum of B. The result is consistent with the conclusion of the recent review [37]. For C, it is blue-shifted by 16 nm compared with B and red-shifted by 11 nm compared with A. This can be explained as follows: the methoxycarbonyl group, being the electron withdrawing substituent, decreases the electron density of the dithiolene moiety as compared with B. When compared with A, the methoxycarbonyl group of C increases the conjugation of the whole molecular plane and extends π delocalization. The results show that the λ_{max} of nickel bis(dithiolene) complexes are effected by the substituted groups, which are the integration of conjugation effect, induction effect and field effect. On the other hand, the absorption spectra of D in solution and on TiO_2 film were shown in Fig. 4b. Both the spectra of D in solution and on TiO_2 film showed intense and broad absorptions centered at around 890 nm in the NIR region. When the dye was deposited on TiO_2 film, the absorption band became broader and the maximum absorption data slightly shifted to a longer wavelength region. This can be attributed to the aggregation of the dyes on the surface of TiO_2 film [38].

3.4.3. Spectroelectrochemistry

Fig. 5a displays the general formula of the ligands in nickel bis(dithiolene) complexes. Different from the other complexes, the spectroelectrochemistry of the nickel bis(dithiolene)

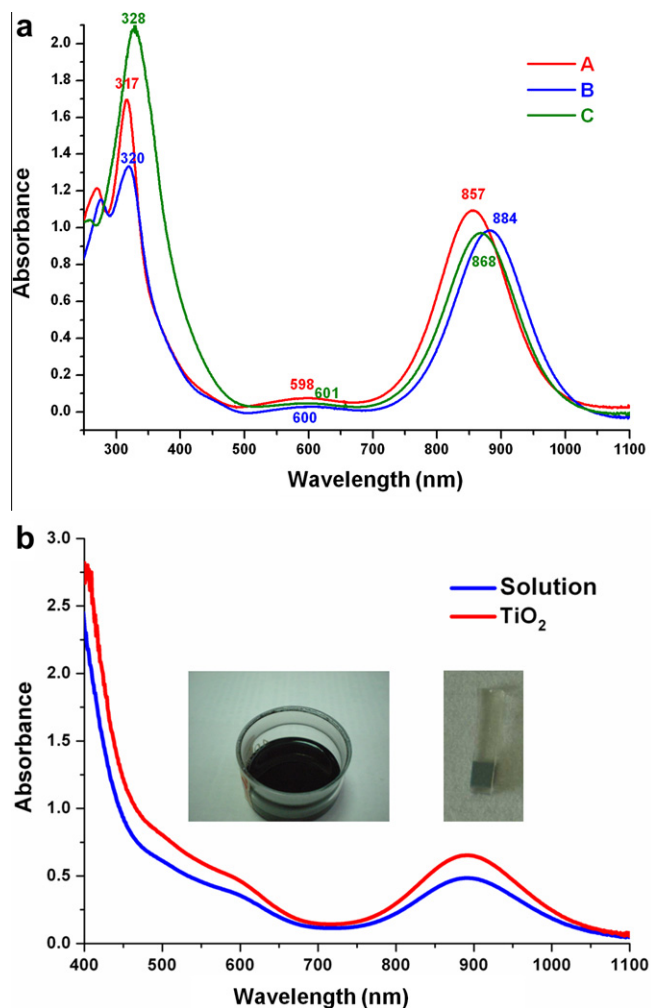


Fig. 4. UV-Vis-NIR spectra of (a) A (red line), B (blue line), and C (green line) in CH₂Cl₂ solution; (b) D in CH₂Cl₂ solution (blue line) and coated on the TiO₂ film (red line). (For interpretation of the references to color in this figure legend, the reader is referred to the web version of this paper.)

Table 1
Maximum absorption data of the three nickel complexes in different solvents.

Samples	Solvents (polarity)						
	Et ₂ O (2.9)	CH ₂ Cl ₂ (3.4)	THF (4.2)	CHCl ₃ (4.4)	Dioxane (4.8)	DMF (6.4)	DMSO (7.2)
Complex A	844	857	856	858	856	871	871
Complex B	869	884	880	883	880	895	896
Complex C	861	868	867	871	869	944	957

complexes is interesting and the absorption spectra of the electrochemically generated mono- and dianions of **A** are shown in Fig. 5b. When the bias is performed, a drastic decrease in the LLCT absorption band with the maxima of 852 nm is observed, which is assigned to the neutral complex **A** ([Ni^{II}(L')(L)]). Its reduced monoanion form [Ni^{II}(L')(L)]⁻, on the other hand, shifts this maxima to 930 nm. The decreased bands at 592 nm, the increased bands near 400 nm, the new band at 529 nm, and the decreased band at 930 nm of the reduced anion form can be observed over time. Subsequently, the corresponding dianion [Ni^{II}(L')(L)]²⁻ is formed

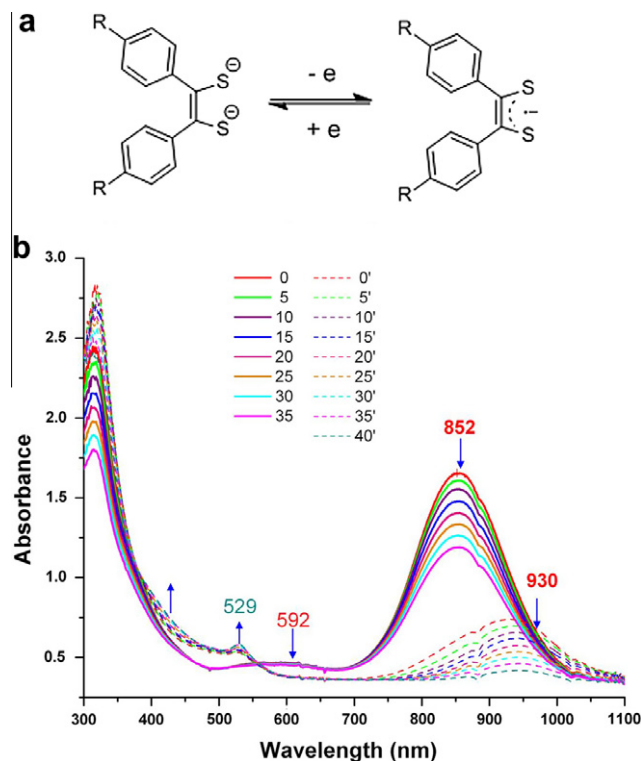


Fig. 5. (a) The general formula of the ligands in nickel bis(dithiolene) complexes; (b) Absorption spectra of neutral **A** (solid line) and its electrochemically generated monoanion and dianion (dotted line) in CH₂Cl₂ solution. The spectra were recorded every 5 s.

nearly without the LLCT absorption [39]. This behavior is similar to those reduced forms of square-planar bis(benzene-1,2-dithiolato) metal complexes [35] and is consistent with the results that the absorption intensity in the NIR region of neutral complexes is generally weakened upon oxidation or reduction [40,41].

3.5. Electrochemical properties

In Fig. 6, cyclic voltammetry and differential pulse voltammetry (CV/DPV) are applied to study the electron exchange in the complexes. With excellent reversibility, three pairs of reversible redox waves are observed, as shown in Fig. 6a and b. The peaks in Fig. 6a (from left to right) are assigned to the couples of [A]¹⁺/[A]⁰, [A]⁰/[A]¹⁻ and [A]¹⁻/[A]²⁻. The same conclusion can be made for B [5,42,43]. It is known that the first oxidation potential corresponds to the HOMO level of the dye [44]. The HOMO levels of **A** and **B** can be obtained by using ferrocene as an internal standard [45]. The values are 5.40 and 5.29 eV for **A** and **B**, respectively.

Fig. 6c shows the mono- and dielectron reduction of **A**, **B** and **C**. The reversible peaks near 0 V show the mono-electron reduction of the complexes with the half-wave potentials of $E_{1/2(A)}^1 = 0.11$ V, $E_{1/2(B)}^1 = 0.05$ V and $E_{1/2(C)}^1 = 0.24$ V for **A**, **B** and **C**. In the same way, the values of the dielectron reduction can be obtained as follows: $E_{1/2(A)}^2 = -0.72$ V, $E_{1/2(B)}^2 = -0.78$ V and $E_{1/2(C)}^2 = -0.54$ V. These values are consistent with the results of DPV (Fig. 6d). Fig. 6c also reveals the substituent effect of different groups on the redox potentials. It is interesting to find that the complexes are oxidized in the following order: **B**, **A**, **C**. The potentials of **B** are the most negative, which can be explained by the fact that the electron density at the center core is slightly increased due to the electron-donating property of methyl groups. Thus, among the three complexes, **B** can be oxidized most easily. With the

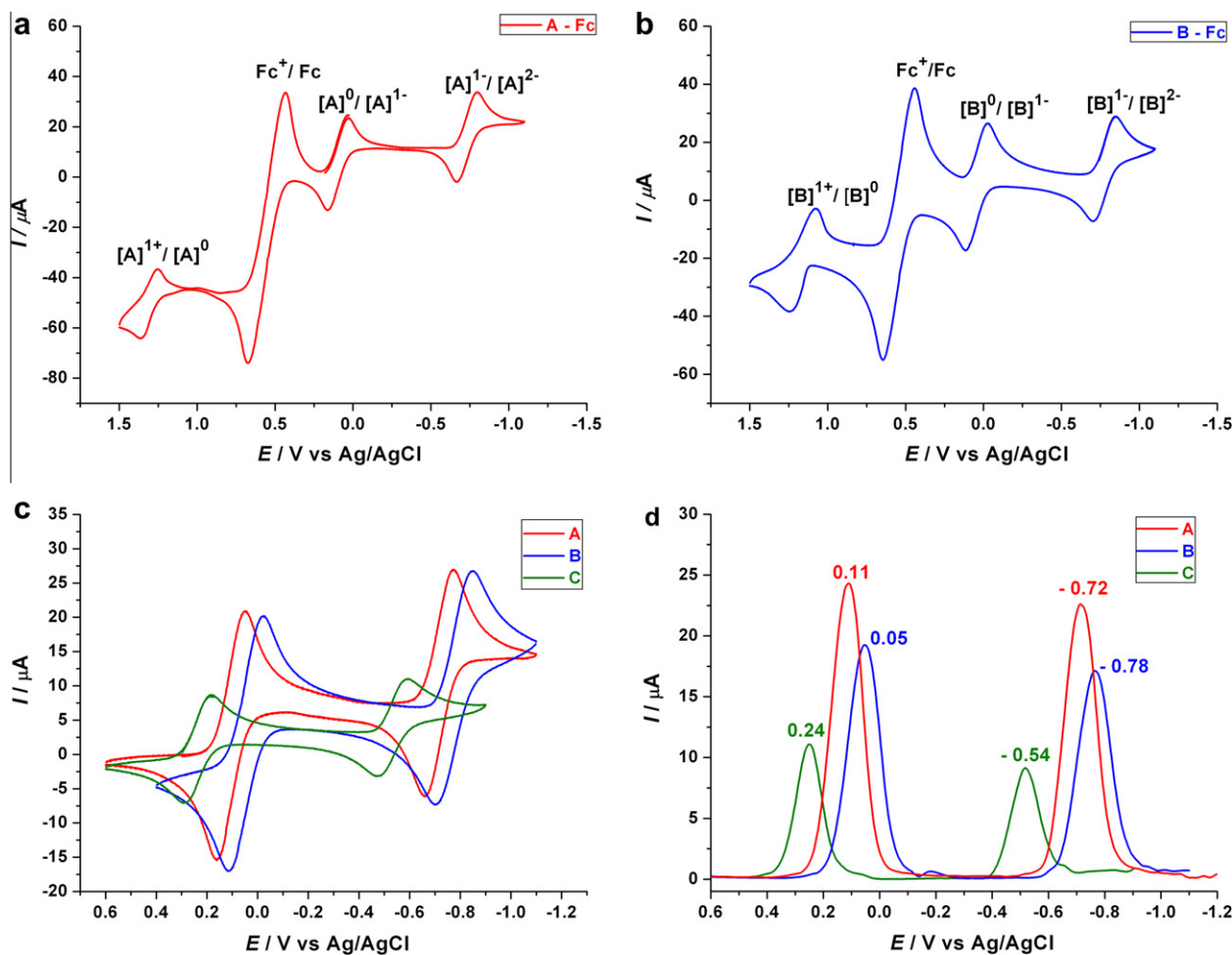


Fig. 6. Cyclic voltammograms of (a) A and (b) B with Fc^+/Fc ; (c) Cyclic voltammograms and (d) differential pulse voltammograms of A (red line), B (blue line) and C (green line) in CH_2Cl_2 . (For interpretation of the references to color in this figure legend, the reader is referred to the web version of this paper.)

electron-withdrawing group, C is the most difficult to oxidize, due to the decreased electron density.

3.6. DFT calculations

Fig. 7 shows the geometric and electronic properties of the dyes performed with DFT calculations. The LUMO and HOMO energy levels (E_{LUMO} and E_{HOMO}) are obtained. The E_{LUMO} are 3.79, 3.65, 4.16 and 4.27 eV for A, B, C and D, with the corresponding E_{HOMO} values of 5.34, 5.16, 5.73 and 5.85 eV, respectively. These results are consistent with the substituent effect. The electron-donating group increases the electron density of the dithiolenic moiety with the higher values of E_{HOMO} and E_{LUMO} , but more improvement is obtained for E_{HOMO} . Thereby the gap of HOMO and LUMO is decreased [5]. The electron distribution in the figure further validates the planar structure and delocalized π -electrons of the complexes. The electrons are distributed on both the dithiolenic moiety and the phenyl ring for HOMO. During electronic excitation at LUMO level, the electrons move from the ligands to the nickel plane. The different substituent groups affect the electron density in the phenyl ring, with increased electron density for electron-donating group and decreased electron density for electron-withdrawing group. Furthermore, the HOMO levels of DFT are approximate to the values obtained by CV. For A, E_{HOMO} by DFT was 5.34 eV, with the E_{HOMO} of 5.40 eV by CV. For B, the HOMO level was 5.16 eV by DFT, with the E_{HOMO} of 5.29 eV by CV. The results show that there is consistency between DFT and CV.

3.7. Applications

3.7.1. DSCs

The NIR dyes of A, B, C and D were applied to fabricate DSCs. The I - V curves are shown in Fig. 8. The open circuit voltage (V_{OC}) of the cell A, B, C, and D were 433, 454, 424, and 411 mV, respectively. The short circuit current density (J_{SC}) of 0.32, 0.32, 0.55, and 0.51 mA/cm^2 were obtained for cell A, B, C, and D, and the energy conversion efficiencies were in the range of 0.07–0.11%. The imperfect performance of DSCs based on nickel bis(dithiolenic) complexes can be attributed to the following reasons: First, the efficiencies of DSCs based on NIR dyes are usually low due to the lower energy of the NIR light. Second, for cell A, B and C, it is the lack of chemical bonds between the dyes and TiO_2 [46], which can stimulate the excited electrons of dye to effectively inject into the conduction band of TiO_2 . As for D with COOH group, in spite of the bond between dye and TiO_2 , the energy level of the complex cannot well match that of the DSC system. The LUMO of the dye used in DSC must be higher than the conduction band of TiO_2 ($E_{\text{CB}} = 3.9\text{--}4.2$ eV [47,48]) and the HOMO level should be lower than the redox potential of I^-/I_3^- (4.85 eV) [47]. The subsequent DFT calculations also show that the LUMO level of D is 4.27 eV. This value is similar to the E_{CB} of TiO_2 and the excited electrons of D cannot be injected effectively into the E_{CB} of TiO_2 . As a result, the electron cycle in the DSC system cannot possibly be proceeded, therefore resulting in the low J_{SC} and the efficiency. Third, the DFT results show a high localization of the electrons in the metallic ring plane

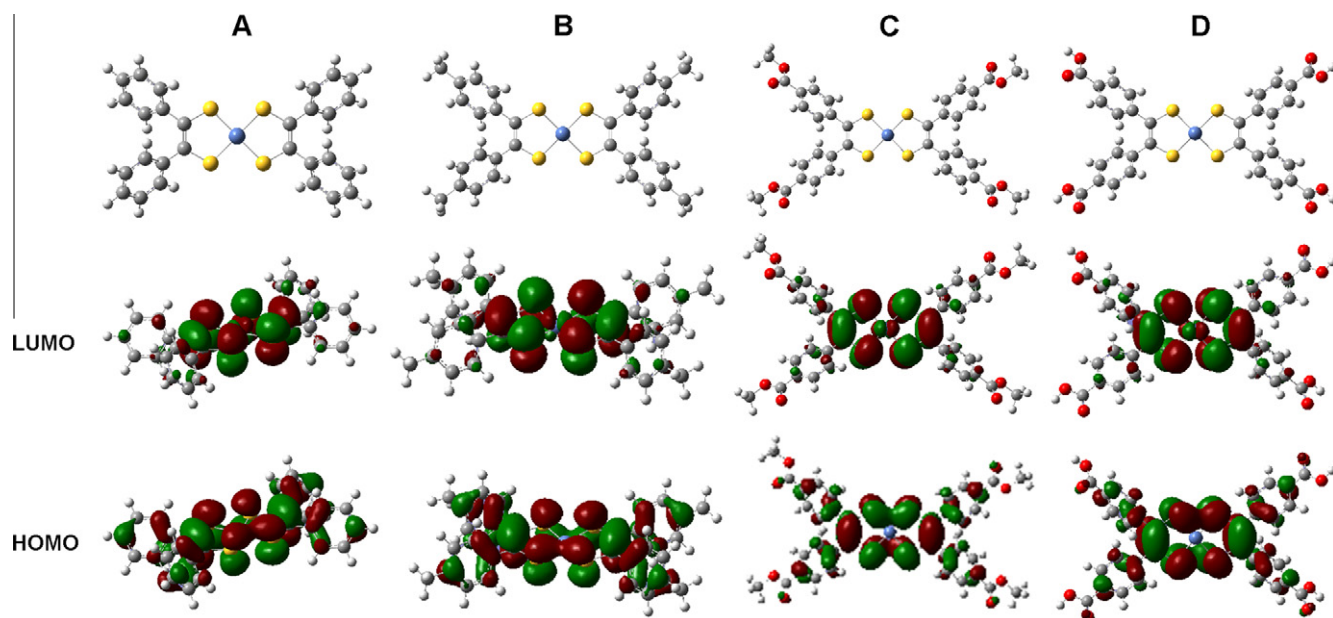


Fig. 7. Frontier molecular orbital pictures of A, B, C and D base on DFT/B3LYP.

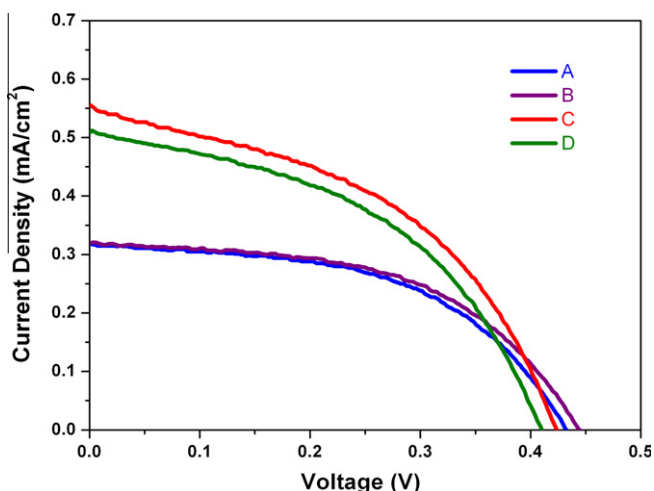


Fig. 8. *I*–*V* curves of the DSCs based on A, B, C and D.

of the nickel bis(dithiolene) complexes, which is unfavorable for charge separation. In general, for effective electron injection and charge separation, the electrons at LUMO should distribute near the COOH groups [49]. Although we introduced the electron withdrawing substituent groups of COOMe and COOH into the structure, the symmetrical structures and the high localization of the electrons of C and D reduces the electron withdrawing ability. Our results demonstrated that the nickel bis(dithiolene) complexes are promising NIR dyes due to their particular photoelectrochemical properties, however, to further improve the efficiency of DSCs, it is necessary to modify the energy levels and the structures of dithiolene complexes, such as changing metal center, introducing stronger electron withdrawing group, and developing unsymmetrical structure. The related work is in progress.

3.7.2. The NIR absorbing filters

The transmittance spectra of the NIR absorbing filter based on complex A (PMMA-A) was shown in Fig. 9. It can be clearly seen that there is no absorption band between 400 and 1100 nm in

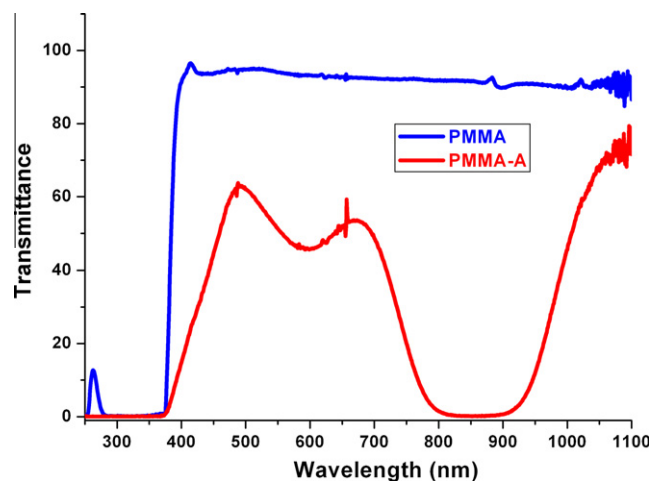


Fig. 9. Transmittance spectra of PMMA (blue line) and the NIR absorbing filters based on PMMA-A (red line). (For interpretation of the references to color in this figure legend, the reader is referred to the web version of this paper.)

the spectrum of PMMA. The green NIR absorbing filter based on PMMA-A showed strong and broad absorption band in the range of 700–1000 nm. In other words, the fabricated NIR absorbing filter can effectively filter the NIR light in the range of 700–1000 nm. This is very useful in many optical devices for martial applications, such as filtering the interferential light of the light-emitting device to the Night Vision Imaging System (NVIS) – compatible lighting. With the superior properties, such as good photothermal stability, excellent solubility, low toxicity, the nickel bis(dithiolene) complex exhibits the great potential in the application of NIR absorbing filters.

4. Conclusions

We synthesized several nickel bis(dithiolene) complexes with strong and broad absorptions in the NIR region (700–1100 nm). The structure, optical spectroscopy, and electrochemical properties

of these dyes were systematically studied. These NIR dyes were first applied to DSCs and the photovoltaic performances of the devices were investigated. With the essential characters of dyes used in DSCs, such as high molar extinction coefficients and excellent reversibility, the nickel bis(dithiolene) complexes exhibit the potential for application in DSC. We found that the structure and the proper energy level of the dyes are important factors that affect the efficiency of DSCs. Although the efficiencies of the fabricated DSCs are unsatisfied, our results are useful and helpful for designing and modifying the structures of dyes to further improve the efficiencies of DSCs based on the NIR dyes. There is also another possibility for the NIR dyes with the visible dyes to be used in tandem DSCs, hybrid DSCs and co-sensitized DSCs. Furthermore, the great potential of the synthesized complexes for the application of NIR absorbing filters is verified. With their particular photoelectrochemical properties, the nickel bis(dithiolene) complexes exhibit promising prospects for future application.

Acknowledgments

This research is financially supported by the National Natural Science Foundation of China (No. 50773008) and the National High Technology Research and Development Program for Advanced Materials of China (No. 2009AA03Z220).

Appendix A. Supplementary material

CCDC 814307 contains the supplementary crystallographic data for B this paper. These data can be obtained free of charge from The Cambridge Crystallographic Data Centre via www.ccdc.cam.ac.uk/data_request/cif. Supplementary data associated with this article can be found, in the online version, at [doi:10.1016/j.ica.2011.07.046](https://doi.org/10.1016/j.ica.2011.07.046).

References

- [1] G.N. Schrauzer, V. Mayweg, *J. Am. Chem. Soc.* 84 (1962) 3221.
- [2] W. Paw, R. Eisemberg, *Inorg. Chem.* 36 (1997) 2287.
- [3] P.L. Hill, L.Y. Lee, T.R. Younkin, S.D. Orth, L.M. White, *Inorg. Chem.* 36 (1997) 5655.
- [4] D. Belo, M. Almeida, *Coord. Chem. Rev.* 254 (2010) 1479.
- [5] T.T. Bui, B. Garreau-de Bonneval, K.I. Moineau-Chane Ching, *New J. Chem.* 34 (2010) 337.
- [6] J.Y. Cho, B. Domercq, S.C. Jones, J.S. Yu, X.H. Zhang, Z.S. An, M. Bishop, S. Barlow, S.R. Marder, B. Kippelen, *J. Mater. Chem.* 17 (2007) 2642.
- [7] M.C. Aragoni, M. Arca, F.A. Devillanova, F. Isaia, V. Lippolis, A. Mancini, L. Pala, G. Verani, T. Agostinelli, M. Caironi, D. Natali, M. Sampietro, *Inorg. Chem. Commun.* 10 (2007) 191.
- [8] K.H. Drexhage, G.A. Reynolds, *Opt. Commun.* 10 (1974) 18.
- [9] H. Shiozaki, H. Nakazumi, *Bull. Chem. Soc. Jpn.* 63 (1990) 265.
- [10] H. Shiozaki, H. Nakazumi, *Bull. Chem. Soc. Jpn.* 63 (1990) 2653.
- [11] I.H. Song, C.H. Rhee, S.H. Park, S.L. Lee, D. Grudinin, K.H. Song, J. Choe, *Org. Process Res. Dev.* 12 (2008) 1012.
- [12] H. Shiozaki, H. Nakazumi, T. Kitao, *J. Soc. Dyers Colour.* 104 (1988) 173.
- [13] S. Oliver, C. Winter, *Adv. Mater.* 4 (1992) 119.
- [14] C.S. Winter, S.N. Oliver, J.D. Rush, C.A.S. Hill, A.E. Underhill, *Mol. Cryst. Liq. Cryst.* 235 (1993) 181.
- [15] G.C. Anyfantis, G.C. Papavassiliou, N. Assimomytis, A. Terzis, V. Psycharis, C.P. Raptopoulou, P. Kyritsis, V. Thoma, I.B. Koutselas, *Solid State Sci.* 10 (2008) 1729.
- [16] T.D. Anthopoulos, G.C. Anyfantis, G.C. Papavassiliou, D.M. de Leeuw, *Appl. Phys. Lett.* 90 (2007) 122105.
- [17] T.D. Anthopoulos, S. Setayesh, E. Smits, M. Cölle, E. Cantatore, B. de Boer, P.W.M. Blom, D.M. de Leeuw, *Adv. Mater.* 18 (2006) 1900.
- [18] T. Taguchi, H. Wada, T. Kambayashi, B. Noda, M. Goto, T. Mori, K. Ishikawa, H. Takezoe, *Chem. Phys. Lett.* 421 (2006) 395.
- [19] B. O'Regan, M. Grätzel, *Nature* 353 (1991) 737.
- [20] H.J. Snaith, *Adv. Funct. Mater.* 20 (2010) 13.
- [21] Simon Kuster, Frédéric Sauvage, Md.K. Nazeeruddin, Michael Grätzel, Frank A. Nüesch, Thomas Geiger, *Dyes Pigments* 87 (2010) 30.
- [22] Shogo Mori, Morio Nagata, Yuki Nakahata, Kazumasa Yasuta, Ryota Goto, Mutsumi Kimura, Minoru Taya, *J. Am. Chem. Soc.* 132 (2010) 4054.
- [23] T. Yamaguchi, Y. Uchida, S. Agatsuma, H. Arakawa, *Sol. Energy Mater. Sol. Cells* 93 (2009) 733.
- [24] F. Inakazu, Y. Noma, Y. Ogomi, S. Hayase, *Appl. Phys. Lett.* 93 (2008) 093304.
- [25] D.B. Kuang, P. Walter, F. Nüesch, S. Kim, J. Ko, P. Comte, S.M. Zakeeruddin, M.K. Nazeeruddin, M. Grätzel, *Langmuir* 23 (2007) 10906.
- [26] Q.Q. Miao, L.Q. Wu, J.N. Cui, M.D. Huang, T.L. Ma, *Adv. Mater.* 23 (2011) 2764.
- [27] R. Breslow, *J. Am. Chem. Soc.* 80 (1958) 3719.
- [28] G.N. Schrauzer, V.P. Mayweg, *J. Am. Chem. Soc.* 87 (1965) 1483.
- [29] B. Mohr, V. Enkelmann, G. Wegner, *J. Org. Chem.* 59 (1994) 635.
- [30] K. Sung, R.H. Holm, *J. Am. Chem. Soc.* 124 (2002) 4312.
- [31] M.H. Petersen, S.A. Gevorgyan, F.C. Krebs, *Macromolecules* 41 (2008) 8986.
- [32] F. Akutsu, M. Inoki, K. Sunouchi, Y. Sugama, Y. Kasashima, K. Naruchi, M. Miura, *Polymer* 39 (1998) 1637.
- [33] T. Ma, T. Kida, M. Akiyama, *Electrochem. Commun.* 5 (2003) 369.
- [34] R. Perochon, L. Piekara-Sady, W. Jurga, R. Clérac, M. Fourmigué, *Dalton Trans.* (2009) 3052.
- [35] K. Ray, T. Weyhermüller, F. Neese, K. Wieghardt, *Inorg. Chem.* 44 (2005) 5345.
- [36] H. Shiozaki, H. Nakazumi, Y. Nakado, *Chem. Lett.* (1987) 2393.
- [37] B.G. Bonneval, K.I. Moineau-Chane Ching, F. Alary, T.-T. Bui, L. Valade, *Coord. Chem. Rev.* 254 (2010) 1457.
- [38] Xiao-Feng Wang, Osamu Kitao, Haoshen Zhou, Hitoshi Tamiaki, Shin-ichi Sasaki, *J. Phys. Chem. C* 113 (2009) 7954.
- [39] S. Kokatam, K. Ray, J. Pap, E. Bill, W.E. Geiger, R.J. LeSuer, P.H. Rieger, T. Weyhermüller, F. Neese, K. Wieghardt, *Inorg. Chem.* 46 (2007) 1100.
- [40] P. Chaudhuri, C.N. Verani, E. Bill, E. Bothe, T. Weyhermüller, K. Wieghardt, *J. Am. Chem. Soc.* 123 (2001) 2213.
- [41] D. Herebian, E. Bothe, E. Bill, T. Weyhermüller, K. Wieghardt, *J. Am. Chem. Soc.* 123 (2001) 10012.
- [42] G.C. Papavassiliou, G.C. Anyfantis, C.P. Raptopoulou, V. Psycharis, N. Ioannidis, V. Petrouleas, P. Paraskevopoulou, *Polyhedron* 28 (2009) 3368.
- [43] S.S. Alix, G.B. Bénédicte, I.C. Kathleen, V. Lydie, *J. Electroanal. Chem.* 624 (2008) 84.
- [44] Z. Kong, H. Zhou, J. Cui, T. Ma, X. Yang, L. Sun, J. Photochem. Photobiol. A: Chem. 213 (2010) 152.
- [45] Robert R. Gagné, Carl A. Koval, George C. Lisensky, *Inorg. Chem.* 19 (1980) 2855.
- [46] T. Ma, K. Inoue, H. Noma, K. Yao, E. Abe, *J. Photochem. Photobiol. A: Chem.* 152 (2002) 207.
- [47] F. Lenzmann, J. Krueger, S. Burnside, K. Brooks, M. Grätzel, D. Gal, S. Rühle, D. Cahen, *J. Phys. Chem. B* 105 (2001) 6347.
- [48] A. Hagfeldt, G. Boschloo, L. Sun, L. Klöö, H. Pettersson, *Chem. Rev.* 110 (2010) 6595.
- [49] M.K. Nazeeruddin, F.D. Angelis, S. Fantacci, A. Selloni, G. Viscardi, P. Liska, S. Ito, B. Takeru, M. Grätzel, *J. Am. Chem. Soc.* 127 (2005) 16835.